Herbicide-Induced Changes in Charge Recombination and Redox Potential of Q_A in the T4 Mutant of *Blastochloris viridis*†

C. Fufezan,*,‡,§ F. Drepper,‡ H. D. Juhnke,|| C. R. D. Lancaster,|| S. Un,§ A. W. Rutherford,§ and A. Krieger-Liszkay‡

Institut für Biologie II, Biochemie der Pflanzen, Universität Freiburg, Schänzlestrasse 1, 79104 Freiburg, Germany, Service de Bioénergétique, DBJC, CNRS URA 2096, CEA Saclay, 91191 Gif-sur-Yvette Cedex, France, and Department of Molecular Membrane Biology, Max Planck Institute of Biophysics, Max-von-Laue-Strasse 3, 60438 Frankfurt am Main, Germany

Received January 11, 2005; Revised Manuscript Received February 22, 2005

ABSTRACT: To gain new insights into the function of photosystem II (PSII) herbicides DCMU (a urea herbicide) and bromoxynil (a phenolic herbicide), we have studied their effects in a better understood system, the bacterial photosynthetic reaction center of the terbutryn-resistant mutant T4 of *Blastochloris* (*Bl.*) *viridis*. This mutant is uniquely sensitive to these herbicides. We have used redox potentiometry and time-resolved absorption spectroscopy in the nanosecond and microsecond time scale. At room temperature the $P^{+\bullet}Q_A^{-\bullet}$ charge recombination in the presence of bromoxynil was faster than in the presence of DCMU. Two phases of $P^{+\bullet}Q_A^{-\bullet}$ recombination were observed. In accordance with the literature, the two phases were attributed to two different populations of reaction centers. Although the herbicides did induce small differences in the activation barriers of the charge recombination reactions, these did not explain the large herbicide-induced differences in the kinetics at ambient temperature. Instead, these were attributed to a change in the relative amplitude of the phases, with the fast:slow ratio being ∼3:1 with bromoxynil and ∼1:2 with DCMU at 300 K. Redox titrations of Q_A were performed with and without herbicides at pH 6.5. The E_m was shifted by approximately −75 mV by bromoxynil and by approximately +55 mV by DCMU. As the titrations were done over a time range that is assumed to be much longer than that for the transition between the two different populations, the potentials measured are considered to be a weighted average of two potentials for Q_A. The influence of the herbicides can thus be considered to be on the equilibrium of the two reaction center forms. This may also be the case in photosystem II.

The first steps of biological conversion of sunlight into chemical energy take place in large transmembrane protein complexes known as reaction centers. Light is absorbed by pigments, and the energy absorbed is transduced into chemical energy in the form of a transmembrane charge separation over a series of cofactors within the reaction center. In the purple bacterial reaction center a pair of bacteriochlorophylls (P)[1] undergoes excitation and oxidation with the ejected electron being transferred via a monomeric bacteriochlorophyll and a bacteriopheophytin (BPheo) to the primary quinone, Q_A, and finally to a secondary quinone, Q_B. Q_A is a one-electron carrier while Q_B is able to undergo two sequential one-electron reduction steps, the second of which is accompanied by protonation, before the fully reduced and protonated quinol is released from its site in exchange for a ubiquinone from the pool in the membrane (*1*−*3*).

The detailed atomic structure of the reaction center has been obtained in several species including *Blastochloris* (*Bl.*) *viridis* (formerly known as *Rhodopseudomonas viridis*) (*4*) and *Rhodobacter* (*Rb.*) *sphaeroides* (*5*). Both types of reaction centers are formed by three polypeptide subunits, L, M, and H, while *Bl. viridis* has an additional C subunit (39.7 kDa). The L and M subunits have a molecular mass of 30.4 and 35.9 kDa, respectively. They form a pseudo-symmetrical dimer that noncovalently binds all of the cofactors needed for charge separation. The H subunit (28.5 kDa) caps the complex on the periplasmic side and provides channels for the protonation of the second quinone acceptor, Q_B. The C subunit found in *Bl. viridis* contains four covalently attached hemes that donate electrons to the oxidized primary electron donor $P^{+\bullet}$. The four hemes get reduced by the mobile electron carrier cytochrome c_2 or a high-potential iron−sulfur protein (HiPIP). These proteins shuttle electrons from the cytochrome bc_1 complex to the reaction center as a part of the cyclic electron pathway (*6*).

Although the overall structural homologies between the reaction centers of *Bl. viridis* and *Rb. sphaeroides* are very

† The financial support of the Universität Freiburg/DAAD, Marie Curie Training Site Specbio, the Volkswagen Stiftung, and Marie Curie Research Network Intro2 is gratefully acknowledged.

* To whom correspondence should be addressed. Tel: ++33-(0)1.69.08.8657. Fax: ++33-(0)1.69.08.8717. E-mail: fufezan@cea.fr.

‡ Universität Freiburg.

§ CNRS URA 2096, CEA Saclay.

|| Max Planck Institute of Biophysics.

[1] Abbreviations: DCMU, 3-(3,4-dichlorophenyl)-1,1-dimethylurea; BRC, bacterial reaction center; PSII, photosystem II; P, primary electron donor; Q_A, primary quinone electron acceptor; Q_B, secondary quinone electron acceptor; BPheo, bacteriopheophytin (the primary electron acceptor in bacteria); Pheo, pheophytin (primary electron acceptor in PSII).

10.1021/bi050055j CCC: $30.25
Published on Web 03/25/2005

high, the charge recombination reaction between $P^{+\bullet}$ and $Q_A^{-\bullet}$ exhibits completely different physical behavior. In *Rb. sphaeroides* the reaction is slow, is temperature-independent at ambient temperatures, and involves a direct tunneling pathway, while in *Bl. viridis* the dominant recombination is rapid, is thermally activated, and involves the reversal of some of the forward electron transfer steps (*7*). This activated pathway is thought to occur via a relaxed form of the $[P^{+\bullet}BPheo^{-\bullet}]$ radical pair designated $[P^{+\bullet}BPheo^{-\bullet}]_\rho$. The free energy gap ΔG between the radical pairs $[P^{+\bullet}BPheo^{-\bullet}]_\rho$ and $[P^{+\bullet}Q_A^{-\bullet}]$ determines which of the recombination pathways dominates (*8*, *9*). The smaller energy gap in *Bl. viridis* results from the presence of a lower potential quinone, a menaquinone, as Q_A compared to ubiquinone in *Rb. sphaeroides* and a higher potential BPheo *b* as compared to a BPheo *a* in *Rb. sphaeroides* (*10*). It seems also likely that the amino acid composition of the Q_A and BPheo sites contributes to the differences in the energy gap between the two species.

Photosystem II (PSII), the water oxidizing reaction center of cyanobacteria and higher plants, is similar in many respects to the purple bacterial reaction center, and this is particularly marked for the electron acceptor components (*11*, *12*). A number of herbicides bind to the Q_B site blocking forward electron transfer (*13*, *14*) and thus favoring back-reactions involving $Q_A^{-\bullet}$. Phenolic and urea herbicides have the opposite effect on the E_m of Q_A in that they induce negative and positive shifts of about -45 and $+50$ mV, respectively (*15*, *16*). By analogy to the situation described above in bacterial reaction centers, the lowering of the Q_A potential induced by phenolic herbicides is thought to favor the back-reaction via the $[P^{+\bullet}Pheo^{-\bullet}]_\rho$ intermediate, while the higher potential induced by urea herbicides favors the direct recombination route (*15*−*18*). Since in PSII the $[P^{+\bullet}Pheo^{-\bullet}]$ route involves chlorophyll triplet (^3P) formation (*19*, *20*) and since ^3P is at an energy high enough to react with O_2 and produce singlet oxygen (*21*−*26*), it has been suggested that this pathway redistribution could explain the enhanced photodamage associated with the herbicidal properties of phenolic herbicides (*15*, *16*). The molecular origin of these herbicide-induced effects, however, remains unknown.

It has been known for many years that changes in the Q_B site (such as the binding of inhibitors) influence the properties of Q_A (*3*, *27*) and conversely that mutations around Q_A can affect the binding of inhibitors that bind in the Q_B site (*28*, *29*). The reaction center structure shows that the quinone sites are effectively "wired" together, with imidazoles H-bonding the quinones and ligating the non-heme iron on each side of the reaction center. However, exactly how the changes in one site are transferred to the other remains unclear (see ref *30*).

The purple bacterial reaction centers are much simpler systems for study compared to PSII, and they have provided many key insights in the current understanding of PSII (*12*, *31*, *32*). Although some herbicides do bind to the bacterial reaction center, phenolic and urea herbicides do not. Therefore, up to now no experiments relevant to phenolic herbicides have been reported. The T4 mutant of *Bl. viridis*, a selected strain resistant to the triazine herbicide, terbutryn (*28*), is exceptional in that it is sensitive to these PSII specific herbicides (*33*). This unique feature is due to a single mutation within the Q_B pocket, YL222F (*28*), which widens the entrance to the pocket and renders it therefore more accessible (*34*).

Here we have studied the influences of the binding of a urea and a phenolic herbicide on the T4 mutant of *Bl. viridis*, focusing on the recombination reactions and the redox potential of Q_A.

MATERIALS AND METHODS

The herbicide-resistant mutant T4 of *Bl. viridis* was grown as reported earlier (*34*), and chromatophores were isolated as described previously (*35*). Chromatophores were suspended in 50 mM MES and 10 mM KCl, pH 6.0 or 6.5, and sonicated twice for 10 s (0.5 s pulse/1.5 s off) on ice. Dodecyl β-maltoside (0.1% v/v) was added to improve the optical properties prior to the measurements. Glycerol (60% v/v) was added for low-temperature measurements.

Kinetic Measurements. The charge recombination was monitored by the disappearance of the 1280 nm absorption band of $P^{+\bullet}$. The cytochrome hemes were preoxidized to prevent rapid electron donation to $P^{+\bullet}$. This was done either by adding a mixture of ferro/ferricyanide (1:2) in low quantities (<1% v/v) or by adding 100 μM ferricyanide and then washing the sample by several centrifugation steps. The measuring light (OSRAM Xenophot HLX, 24 V, 150 W) was focused with a lens ($f = 100$ mm) onto the sample. Prior to the focusing lens the light was filtered using a heat-reflecting filter (CalFlex X, Balzers), a series of Schott glass filters (OG550 and OG1000), and a monochromating interference filter (Dr. Hugo Anders, GmbH; spectral width ~40 nm centered at 1300 nm). The transmission maximum of the interference filter was tuned to 1280 nm by turning it at an angle of 75° relative to the measuring beam. To minimize scattered light from the excitation pulse, the same series of filters (with the exception of the OG1000) was used between the sample and the photodiode (Ge photodiode J16; E. G. and G. Judson). Excitation was performed using a frequency-doubled Nd:YAG laser (Quantel, 532 nm, 5 ns fwhm), and its energy was adjusted using neutral density filters. In front of the sample the excitation beam was scattered by a dispersion glass to ensure homogeneous excitation. The sample was cooled in a liquid nitrogen cryostat (Oxford Instruments). The time resolution was 4 μs. Data acquisition and processing were performed similarly to that described in Drepper et al. (*36*). Fully reproducible kinetics were observed, indicating that the samples were not damaged by the low temperature or by the flashes. A calculated curve was fitted to the data points of the absorption transient using the nonlinear least-squares Marquardt−Levenberg algorithm in the program GNUplot (v.3.5). Another setup was used to investigate the slow phase at ambient temperatures in greater detail; this used a germanium photodiode as detector, and the sample was temperature controlled in a laboratory-made temperature-controlled cuvette holder. The signals were amplified by a low-noise current amplifier (Stanford Research Systems, model SR570) and recorded on a data acquisition system of local design. The latter offered real-time averaging over a programmable number of digitization periods, yielding a logarithmic time base from 1 μs to 10 s. Ten to twenty single flash experiments were averaged in both setups with a repetition rate of 0.1 Hz.

Transient Absorption Detected Redox Potentiometry. The presence of reduced Q_A was estimated from the percentage

of primary pair [$P^{+\bullet}BPheo^{-\bullet}$] charge recombination ($t_{1/2} \sim$ 5 ns) as monitored in the 1300 nm absorption band of $P^{+\bullet}$. Titrations were carried out on chromatophores at a reaction center concentration of approximately 5 μM [$\epsilon_{830} = 300$ mM^{-1} cm^{-1} (*37*)]. The redox mediator mixture was composed of 40 μM *N*,*N*,*N*′,*N*′-tetramethylphenylenediamine, 300 μM ferric chloride, 20 μM Nile blue A, 70 μM 1,4-naphthoquinone, 100 μM Neutral red, 90 μM indigocarmine, and 100 μM sodium anthraquinone-2-sulfate. Quinone mediators with midpoint potentials around the expected E_m of Q_A were not used in the data shown here; however, other experiments showed that they did not change the results (data not shown). The total volume of solutions added to change the redox potential [i.e., freshly prepared dithionite (100 μM) and potassium ferricyanide (100 μM)] was kept low (<5% v/v). The pH was measured after the set of data was collected. Prior to the experiments the samples were incubated with 100 μM potassium ferricyanide for 1 h in darkness. The single flash experiments were spaced by 1−5 min to avoid accumulation of Q_A^- due to charge separation and to allow the mediators to equilibrate the potential. Longer spacing did not alter the results within the accuracy of the measurement. Five to ten single flash experiments were averaged. Transient absorption measurements were started after the redox potential was stable for at least 5 min. Laser-induced absorption spectroscopy on the nanosecond time scale was carried out as described by Gibasiewicz et al. (*38*). Data processing and determination of the amplitude of the very fast phase relative to the whole signal were done using a homemade program. The program determined the edge (t_{-1}) where the flash occurred by comparing the signal-to-noise ratio. The rms noise was calculated over 150 ns, recorded prior the excitation pulse. The edge, where the excitation occurred, was defined as the time where the signal size was three times bigger than the rms noise. The maximum absorption at t_0 was determined by the signal size after the delay time of the detector response ($t_{-1} + 2$ ns). The relevant maximum was then calculated as an average of three points around t_0 and used to normalize the kinetics. The correct scaling was verified visually. Before and after the 1 h dark incubation with ferricyanide, the kinetic traces did not show the 5 ns [$P^{+\bullet}BPheo^{-\bullet}$] phase. These "all-$Q_A$ oxidized" kinetic traces were used to calculate the detector response time and the baseline for further analysis. The signal size or amplitude of the phase representing centers having Q_A oxidized and therefore not decaying with the 5 ns [$P^{+\bullet}BPheo^{-\bullet}$] phase was calculated by averaging over a window of 25 ns starting at $t_0 + 25$ ns. This level was subtracted from the kinetic trace. The resulting trace showed only the 5 ns phase with positive absorption values. The amount of centers recombining rapidly due to the presence of reduced Q_A was then calculated by the 15 ns integral ($t_0 + 2$ ns, $t_0 + 17$ ns). The possible maximum value of this integral was calculated to be 6.31 ns. This value was supported by the values obtained by the scaling factor for a fit with a standard Nernst curve ($n = 1$) through the measured data points. Therefore, by fixing this value, the final mathematical analysis of the redox titration data was only dependent on E_m, as with the maximal expected amplitude for the very fast $P^{+\bullet}BPheo^{-\bullet}$ recombination, the asymptote of the Nernst curve was determined. This value was further used to scale to 100%.

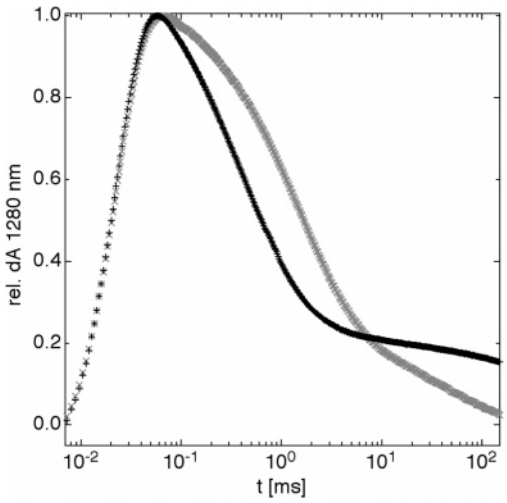

FIGURE 1: Normalized absorption change at 1280 nm due to $P^{+\bullet}$ in chromatophores of the T4 mutant at 298 K on a logarithmic time scale in the presence of 20 μM DCMU (gray trace) or 100 μM bromoxynil (black trace). Fitted parameters are listed in Table 1.

RESULTS

Temperature Dependence of the $P^{+\bullet}Q_A^{-\bullet}$ Charge Recombination Kinetics in the Presence of DCMU or Bromoxynil. Figure 1 shows the decay of the flash-induced $P^{+\bullet}$ in *Bl. viridis* chromatophores at 298 K and pH 6.5 in the presence of DCMU (gray) or in the presence of bromoxynil (black), monitored by its absorption at 1280 nm. At early times $P^{+\bullet}$ reduction is faster in the presence of bromoxynil than in the presence of DCMU. This early part of the decay kinetics shows biphasic behavior. After 10 ms the absorption decay flattens into a very slow phase. In the presence of bromoxynil the reduction of $P^{+\bullet}$ was not complete after the 200 ms observation window. This gives rise to an offset that decays fully between flashes. The data in this time window were, however, adequately described by the sum of three ($n = 3$) exponential functions plus an offset.

$$f_n(x) = A_0 + \sum_{i=1}^{n} A_i \exp(-xk_i) \qquad (1)$$

A_0 is the offset, n is the number of exponentials to fit the $P^{+\bullet}$ reduction, and A_i and k_i are the amplitude and the rate constant of the ith exponential or phase, respectively. The fit was done over the time range 20 μs−150 ms, and the square deviation (χ^2) between the measured data and the calculated fit was in any case smaller than 1% of the signal size within the time window. Fits with less than $n = 3$ for $T > 200$ K and less than $n = 2$ for $T < 200$ K did not sufficiently describe the data (see Supporting Information). The resulting parameters are listed in Table 1. In the following the phases $i = 1$, 2, and 3 are designated fast, slow, and very slow, respectively. The slow phase and the fast phase are attributed to $P^{+\bullet}Q_A^{-\bullet}$ recombination while the very slow phase is attributed to $P^{+\bullet}Q_B^{-\bullet}$ recombination in the fraction of centers in which the herbicides do not bind or were displaced upon arrival of an electron on Q_A [see Stein et al. (*39*) and discussion]. The offset is expected to be made up of a contribution from the slow phase of $P^{+\bullet}Q_B^{-\bullet}$ decay and any longer lived $P^{+\bullet}$ formed for example by the oxidation of reduced quinone by ferricyanide or O_2.

Table 1: Fitted Parameters for the $P^{+\bullet}$ Reduction at 298 K in the Presence of Bromoxynil or DCMU[a]

	bromoxynil			DCMU		
i	A_i (%)	k_i (s^{-1})	$t_{1/2;i}$ (ms)	A_i (%)	k_i (s^{-1})	$t_{1/2;i}$ (ms)
0	14.3			2.8		
1	55.1	2701.0	0.26	24.8	1871.0	0.37
2	24.5	667.1	1.04	54.4	415.9	1.66
3	6.1	17.6	39.4	17.9	25.6	27.1

[a] The phases are notated as i. A_i is the relative amplitude, k_i is the rate constant, and $t_{1/2;i}$ is the corresponding half-time.

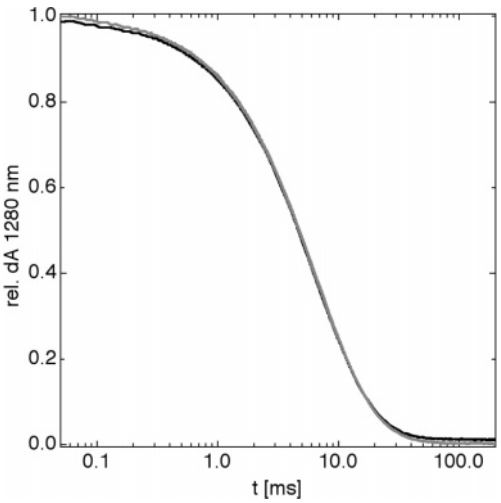

FIGURE 2: Normalized absorption change at 1280 nm due to $P^{+\bullet}$ reduction in chromatophores of the T4 mutant at 80 K on a logarithmic time scale in the presence of 20 μM DCMU (gray trace) or 100 μM bromoxynil (black trace). Fitted parameters are listed in Table 2.

As illustrated in Figure 2, the recombination at low temperature (80 K) showed no differences when DCMU (gray) or bromoxynil (black) was present. A sum of two exponentials ($n = 2$) adequately described the kinetics of $P^{+\bullet}$ reduction at this temperature. The fit parameters for the fast and slow phases ($i = 1, 2$) with their amplitude (A_i), rate constant (k_i), and half-times ($t_{1/2;i}$) are listed in Table 2. The $P^{+\bullet}Q_B^{-\bullet}$ recombination phase is absent because Q_A to Q_B electron transfer is inhibited at low temperature (*40*).

The recombination kinetics were recorded and analyzed in the temperature range from 312 to 80 K. For a clearer presentation of the results from the fits in the presence of the herbicides, they are shown only in the temperature range from 315 to 220 K. The fast and the slow $P^{+\bullet}Q_A^{-\bullet}$ recombinations flatten to a temperature-independent rate constant of 205 ± 15 s^{-1} and 100 ± 10 s^{-1} around 160 and 200 K, respectively. As discussed below, we will focus in this work on the fast and slow phase recombination kinetics. Therefore, the following relative amplitudes and rates do not include the parameters for the offset and the very slow recombination phase that are mainly attributed to the $P^{+\bullet}Q_B^{-\bullet}$ recombination.

Table 2: Fitted Parameters for the $P^{+\bullet}$ Reduction at 80 K in the Presence of Bromoxynil or DCMU[a]

	bromoxynil			DCMU		
i	A_i (%)	k_i (s^{-1})	$t_{1/2;i}$ (ms)	A_i (%)	k_i (s^{-1})	$t_{1/2;i}$ (ms)
0	2.2			0.4		
1	45.8	220	3.1	62	191.5	3.6
2	52.0	112	6.2	37.6	92.1	7.5

[a] The phases are notated as i. A_i is the relative amplitude, k_i is the rate constant, and $t_{1/2;i}$ is the corresponding half-time.

Figure 3 shows the values for the rate constants in the presence of bromoxynil (a, triangles) and DCMU (b, circles) of the fast, k_1 (filled symbols), and the slow, k_2 (open symbols), phases plotted against temperature. As expected for *Bl. viridis* the rates in general increased with increasing temperature. The recombination rate was found to be slightly faster in the presence of bromoxynil than in the presence of DCMU.

Figure 4 shows the fitted values for the relative amplitudes in the presence of bromoxynil (a, triangles) and DCMU (b, circles) for the fast, A_1 (filled symbols), and slow, A_2 (open symbols), phases plotted against temperature. In both cases, the slow phase dominated at low temperature. Its amplitude decreased when the temperature was raised, while the amplitude of the fast phase increased. In the presence of DCMU the amplitude of the slow phase always dominated, accounting for at least 70%, whereas in the presence of bromoxynil the fast phase becomes the dominant phase at $T > 277$ K, and it accounted for nearly 80% of the $P^{+\bullet}Q_A^{-\bullet}$ decay at 303 K.

Transient Absorption Detected Redox Titrations of Q_A. Redox potentiometry in the absence or presence of the

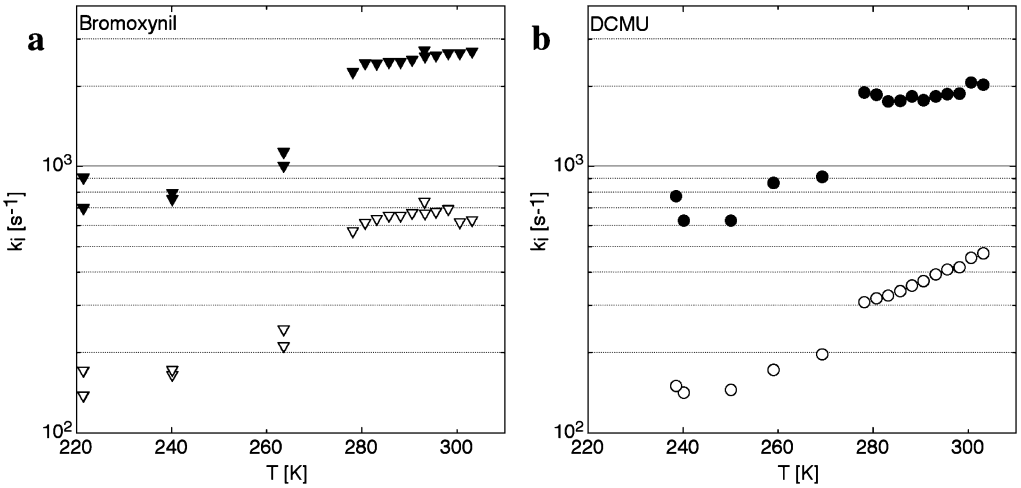

FIGURE 3: Temperature-dependent rate constant of the fast phase (closed symbols) and slow phase (open symbols) in the presence of 100 μM bromoxynil (a) or 20 μM DCMU (b).

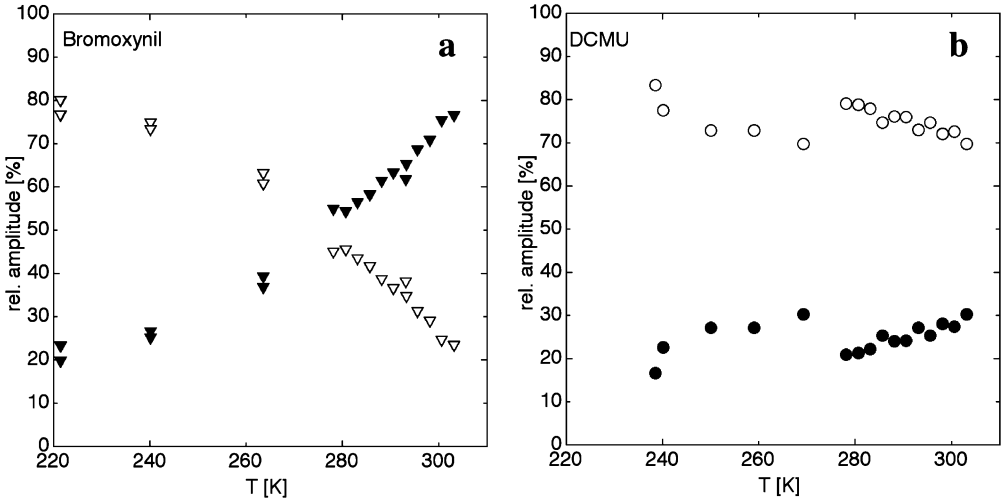

FIGURE 4: Relative distribution of amplitudes of the fast phase (closed symbols) and slow phase (open symbols) vs temperature in the presence of 100 μM bromoxynil (a) or 20 μM DCMU (b). The amplitudes represent the relative amount of centers in which the $P^{+\bullet}Q_A^{-\bullet}$ recombination is fast ($i = 1$) or slow ($i = 2$).

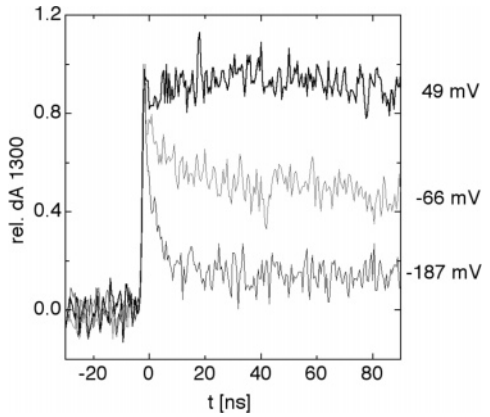

FIGURE 5: Recovery of the 1300 nm absorption due to $P^{+\bullet}$ reduction in T4 chromatophores poised with different potentials. Top to bottom: 49, −66, and −187 mV.

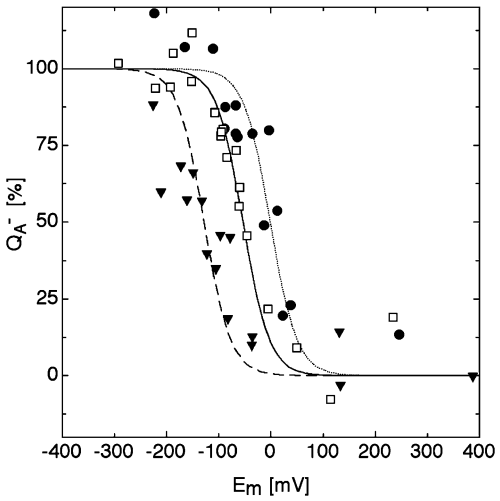

FIGURE 6: Relative amount of reduced Q_A at different redox potentials at pH 6.5 in the presence of DCMU (circles), bromoxynil (triangles), or no addition (squares).

herbicides was carried out at 294 K. The single reduced form of Q_A, the semiquinone ($Q_A^{-\bullet}$), was monitored indirectly by the appearance of the very fast phase of $P^{+\bullet}$ reduction due to $P^{+\bullet}BPheo^{-\bullet}$ recombination with a half-time of about 5 ns (*38*). Its relative amplitude is proportional to the centers with $Q_A^{-\bullet}$. The $P^{+\bullet}$ reduction was monitored at 1300 nm. Figure 5 shows the kinetics of the absorption measured in T4 chromatophores in the absence of herbicides at pH 6.5 and poised at different redox potentials. The kinetic absorption traces shown in Figure 5 from top to bottom were poised at 49, −66, and −187 mV. At 49 mV the absorption did not recover in this short observation window, indicating the presence of relatively stable $P^{+\bullet}$ at this redox potential. This is due to the formation of the $P^{+\bullet}Q_A^{-\bullet}$ radical pair with a half-time in the microsecond to millisecond time range as described above in the temperature-dependent recombination assay. However, at lower potentials, the 5 ns [$P^{+\bullet}BPheo^{-\bullet}$] recombination was observable. The rapid recombination of this radical pair accounts for about 50% of the $P^{+\bullet}$ reduction at −66 mV (middle trace) or more than 85% at −187 mV (lower trace).

We estimated the maximal amplitude of the nanosecond decay due to the fast [$P^{+\bullet}BPheo^{-\bullet}$] recombination within our observation window to be around 90%. The remaining 10% of the decay is probably due to the formation of the triplet state ^3P, which has a longer lifetime and also shows some absorption at 1300 nm (*38*, *41*).

Figure 6 shows the estimated relative concentration of $Q_A^{-\bullet}$ at different redox potentials at pH 6.5 in the presence of bromoxynil (triangles), DCMU (circles), or without addition (squares). Although the signal-to-noise ratio of these measurements is quite low, it is nevertheless clear that the presence of bromoxynil or DCMU differentially modified the midpoint potential of Q_A. Fits of the data with the Nernst equation for a one-electron transition yielded an E_m of −134 ± 25 mV in the presence of bromoxynil, −2 ± 15 mV in the presence of DCMU, and −57 ± 10 mV without any addition, in a Q_B-less state. This represents a shift of approximately +55 ± 25 and −77 ± 35 mV in the presence of DCMU and bromoxynil, respectively, compared to the control, no addition sample, at pH 6.5.

DISCUSSION

We investigated the effect of two PSII herbicides, bromoxynil, a phenolic herbicide, and DCMU, an urea herbicide, in chromatophores of *Bl. viridis* using the T4 mutant. Among purple photosynthetic bacteria this mutant is uniquely sensi-

Table 3: Thermodynamic Parameters Obtained from the Arrhenius Plot of the Fast ($i = 1$) and Slow ($i = 2$) Phase in the Presence of Bromoxynil or DCMU[a]

i		$\Delta H^{\ddagger}$ (eV)	ln A	$\Delta S^{\ddagger}$ (meV·K^{-1})	$\Delta G^{\ddagger}$ (eV)
1	bromoxynil	0.048 ± 0.007	9.695 ± 0.297	-0.613 ± 0.025	0.229 ± 0.015
	DCMU	0.031 ± 0.013	8.663 ± 0.554	-0.702 ± 0.048	0.238 ± 0.028
2	bromoxynil	0.033 ± 0.020	7.625 ± 0.809	-0.792 ± 0.070	0.265 ± 0.041
	DCMU	0.168 ± 0.006	12.359 ± 0.223	-0.384 ± 0.019	0.281 ± 0.011

[a] Activation enthalpy $\Delta H^{\ddagger}$ is the slope divided by the Boltzmann constant, and ln A is the ordinate composed of the entropy and the decay rate of the intermediate state (see eq 3).

tive to these herbicides. We measured (1) the charge recombination over a temperature range from 315 to 80 K and (2) the redox potential of Q_A at pH 6.5.

Recombination Kinetics in the Presence of DCMU or Bromoxynil. The data measured over a temperature range from 315 to 80 K were adequately described by the sum of two or three exponential functions. The phases were attributed to two rates for $P^{+\bullet}Q_A^{-\bullet}$ recombination and one rate for the $P^{+\bullet}Q_B^{-\bullet}$ recombination. The $P^{+\bullet}Q_B^{-\bullet}$ phase was absent at low temperature. The existence of two independent $P^{+\bullet}Q_A^{-\bullet}$ recombination phases is attributed to two populations of reaction centers in different conformational states, in accordance with the literature (*42*−*47*). These two states have been shown to have slightly different absorption spectra (*43*, *44*) and to exist already prior to illumination (*47*).

(A) $P^{+\bullet}Q_B^{-\bullet}$ Recombination. The recombination from $Q_B^{-\bullet}$ occurred in a fraction of the reaction centers because the binding of the herbicide was incomplete. Under the conditions used, which were optimized to monitor $P^{+\bullet}Q_A^{-\bullet}$ recombination, we could not determine the absolute value of the $P^{+\bullet}Q_B^{-\bullet}$ kinetics. However, from the literature it is known that the $P^{+\bullet}Q_B^{-\bullet}$ recombination also exhibits a biphasic character with half-times of about 100 and 350 ms (*48*, *49*). These two phases would contribute to the very slow phase ($i = 3$) and the offset ($i = 0$) in our conditions. The sum of the amplitudes of these two phases is similar in the presence of bromoxynil or DCMU. Sinning et al. (*33*) estimated the IC_{50} of DCMU and ioxynil, the iodinated derivative of bromoxynil, in the T4 mutant to be 8 and ∼100 μM, respectively. The comparison to our result would then indicate a higher affinity of bromoxynil than ioxynil toward the Q_B site of T4.

(B) $P^{+\bullet}Q_A^{-\bullet}$ Charge Recombination. The investigation of the temperature dependency of the recombination kinetics provides information about the energy levels of the radical pairs in the presence of the herbicides for each conformer. In general, the $P^{+\bullet}Q_A^{-\bullet}$ recombination can occur via two main pathways. In *Bl. viridis*, at higher temperature, the charge recombination occurs mainly via a thermally excited state, a relaxed form of the radical pair $[P^{+\bullet}BPheo^{-\bullet}]_\rho$. At lower temperature, the electron returns to $P^{+\bullet}$ via a direct tunneling mechanism that is temperature independent. We measured this direct tunneling rate from $Q_A^{-\bullet}$ to $P^{+\bullet}$ in both conformers at 80 K. The tunneling rates were $k_1^T = 205 \pm 15$ s^{-1} and $k_2^T = 100 \pm 10$ s^{-1} for the fast and slow phases, and they were independent of the type of herbicide. The system exhibited these rates already at 200 and 160 K for the slow and fast phases, respectively (data not shown). The origin of the difference in tunneling rate between the conformers could possibly be due to a different redox potential of Q_A in each conformer. However, as the direct tunneling rate over such a long distance is not only dependent on the driving force but also dependent on the reorganization energy and the coupling, which in principle reflects the distance and/or orientation between the acceptor and the donor (*50*), assigning the origin of the difference in the tunneling rate is not trivial.

To determine the energy gap between $[P^{+\bullet}Q_A^{-\bullet}]$ and $[P^{+\bullet}BPheo^{-\bullet}]_\rho$, the decay rate of $[P^{+\bullet}BPheo^{-\bullet}]_\rho$ must be estimated. The measured rate constants at higher temperature are a sum of the rates for the pathways via the intermediate(s) and for that via direct tunneling.

$$k_i = k_i^T + k_d \exp\left(\frac{-\Delta G_i^{\ddagger}}{k_B T}\right) \qquad (2)$$

where k_i^T is the tunneling rate and $\Delta G_i^{\ddagger}$ the activation energy of phase i, k_d the decay rate of $[P^{+\bullet}BPheo^{-\bullet}]_\rho$, k_B the Boltzmann constant, and T the temperature. The activation free energy $\Delta G_i^{\ddagger}$ is equal to the energy difference between the radical pairs $[P^{+\bullet}Q_A^{-\bullet}]$ and $[P^{+\bullet}BPheo^{-\bullet}]_\rho$, the rate-limiting intermediate step in the fast ($i = 1$) or slow ($i = 2$) recombining conformer. To analyze the kinetic data, it is useful to rearrange eq 2 to

$$\ln(k_i - k_i^T) = \frac{-\Delta H_i^{\ddagger}}{k_B T} + \frac{\Delta S_i^{\ddagger}}{k_B} + \ln k_d \qquad (3)$$

where $\Delta H_i^{\ddagger}$ is the activation enthalpy and $\Delta S_i^{\ddagger}$ is the activation entropy of the fast ($i = 1$) or slow ($i = 2$) phase. While $\Delta H_i^{\ddagger}$ is obtained from the slope of the Arrhenius plot, $\Delta S_i^{\ddagger}$ is a part of a sum describing the so-called preexponential factor, which can be derived from the ordinate, $T \rightarrow \infty$, in Table 3, referred to as ln A. It is clear that the decay rate of the intermediate state k_d must be known in order to calculate the thermodynamic parameters, in particular the activation energy $\Delta G_i^{\ddagger}$. A direct measurement of the decay time of the $[P^{+\bullet}BPheo^{-\bullet}]$ radical pair and in particular the relevant relaxed form is not available; however, we assume that k_d is 2×10^7 s^{-1} and that it is the same for both conformers as already discussed in refs *42*, *45*, and *51*. With this approximation one can calculate the thermodynamic parameters by analyzing the Arrhenius plot shown in panels a and b of Figure 7 for the fast ($i = 1$) and slow ($i = 2$) phases, respectively, in the presence of bromoxynil (triangles) and DCMU (circles). The calculated thermodynamic parameters obtained from Figure 7 are listed in Table 3.

The fast phase exhibits an activation energy, $\Delta H^{\ddagger}$, of 48 and 31 meV in the presence of bromoxynil and DCMU, respectively. However, the entropy seems to play an important contribution to the free energy. In the presence of bromoxynil the entropy loss is about -0.61 meV K^{-1} compared to -0.702 meV K^{-1} in the presence DCMU. This

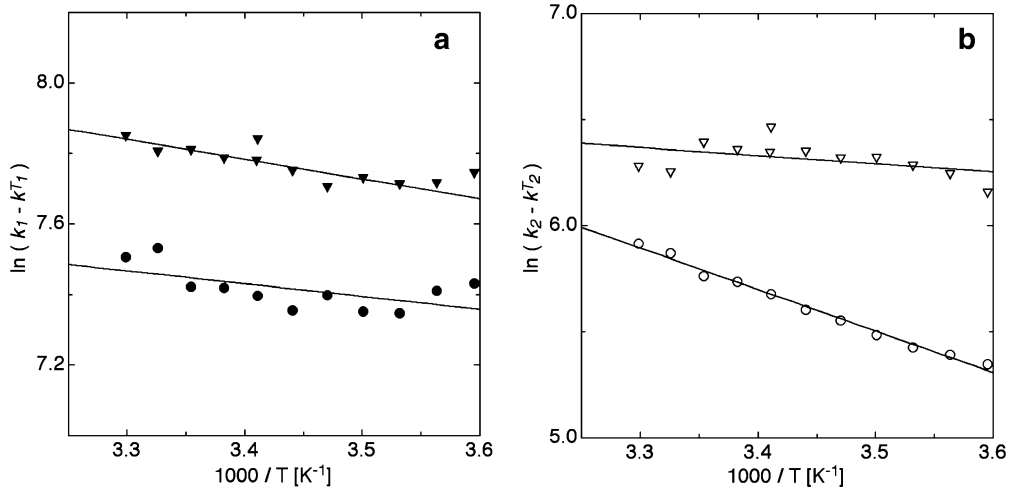

FIGURE 7: Arrhenius plot of the fast phase (a) and slow phase (b) in the presence of 20 μM DCMU (circles) or 100 μM bromoxynil (triangles). The thermodynamic values calculated by the fitted lines are represented in Table 3.

results in only a small herbicide-induced difference in terms of $\Delta G^{\ddagger}$ within the fast conformational state at 293 K. The free energy gap ΔG between $[P^{+\bullet}BPheo^{-\bullet}]_\rho$ and $[P^{+\bullet}Q_A^{-\bullet}]$ is 229 and 238 meV in the presence of bromoxynil and DCMU, respectively.

For the slow phase, reflecting the RC in the slow recombining conformational state, the $\Delta H^{\ddagger}$ is 33 and 170 meV in the presence of bromoxynil and DCMU, respectively. In the presence of DCMU the activation enthalpy is bigger than in the presence of bromoxynil; however, the difference in the loss of entropy, -0.792 and -0.384 meV K^{-1}, in the presence of bromoxynil and DCMU, respectively, compensates this difference. This again results in a very small difference in ΔG within the slow conformational state. The free energy gap ΔG between $[P^{+\bullet}BPheo^{-\bullet}]$ and $[P^{+\bullet}Q_A^{-\bullet}]$ for the slow phase is calculated to be 265 and 281 meV in the presence of bromoxynil and DCMU, respectively.

It seems that the herbicides have only a small influence on the free energy gap between $[P^{+\bullet}BPheo^{-\bullet}]_\rho$ and $[P^{+\bullet}Q_A^{-\bullet}]$ in each conformer, and this makes only a small contribution to overall faster kinetics of recombination when bromoxynil is present. The more marked effect of the herbicide is the change in the amplitudes of the fast (A_1) and slow (A_2) phase. The faster $P^{+\bullet}Q_A^{-\bullet}$ recombination in the presence of bromoxynil is due to a more pronounced faster phase. In the context of the two reaction center conformations ascribed to these two phases in the literature, the herbicide effects are seen as shifting the equilibrium between the two conformers, C_{fast} and C_{slow}.

Previous work has shown that the equilibrium between these conformers was dependent on several parameters. At low pH, low temperature, or high salt concentration, the slow conformation dominates, while at high temperature, higher pH, and higher membrane fluidity, the equilibrium is shifted in favor of the fast phase/conformer (*42*, *43*, *45*−*49*). In the present work we have found that the binding of bromoxynil shifts the equilibrium in favor of the fast conformational state of the reaction center to a ratio of about 2 at 298 K, while the binding of DCMU induces a ratio close to 1:2.

Transient Absorption Detected Redox Titration of Q_A in the Presence of DCMU or Bromoxynil. The redox potential (E_m) of Q_A in the presence of bromoxynil or DCMU and without addition was investigated at pH 6.5. Without any addition we estimated values of -57 ± 10 and -110 ± 15 mV at pH 6.5 and 7.7, respectively. These values show a one-electron per proton behavior, and they correspond well with the E_m values reported for the wild type of *Bl. viridis* of about -60 and -130 mV at pH 6.5 and 7.7, respectively (*52*). At pH 6.5 we measured a shift of $+55 \pm 25$ mV in the presence of DCMU and a shift of -77 ± 35 mV in the presence of bromoxynil. These shifts are remarkably similar to those seen earlier in PSII (*15*).

This herbicide-induced shift of the E_m of Q_A fits with the kinetic data: bromoxynil binding lowers the E_m of Q_A and accelerates charge recombination, whereas DCMU binding increases the Q_A potential and slows charge recombination. The kinetic effects induced by the herbicides are mainly attributed to changes in the ratio of the fast to slow phases of recombination. In this regard we assume that the time scale of the equilibrium redox titration experiment is long compared to the rate of conversion between the two conformational states responsible for the fast and slow phases. Thus the measured E_m values can be taken as representing the average E_ms weighted by the proportions of the two populations present.

This weighted average approach is also supported by the findings in the wild type of *Bl. viridis* already in the literature. In the presence of *o*-phenanthroline, and at pH 6.5, Cogdell and Crofts reported the E_m of Q_A to be around $+60$ mV (*53*) and Sebban and co-workers reported the distribution between the two conformers, C_{fast}:C_{slow}, to be 1:4 (*48*). Our measured ratio of C_{fast}:C_{slow} in the T4 mutant is close to 1:2 in the presence of DCMU, and Q_A shows an E_m of -2 ± 10 mV. A distribution C_{fast}:C_{slow} of 1:1 was observed (*30*) when the reaction centers were depleted of Q_B and reconstituted into lipids. Our titration assays with no addition can also be seen as a Q_B-less condition, because Q_B is reduced before reaching the range of potential where Q_A undergoes reduction, and Q_BH_2 has a low binding affinity for the reaction center. Therefore, our measured ratio C_{fast}:C_{slow} of 1:1 with no addition has a corresponding E_m of Q_A of -57 ± 10 mV. On the other hand, a ratio C_{fast}:C_{slow} of 2:1 in the presence of bromoxynil exhibits an E_m of about -134 ± 20 mV. A clear correlation between the distribution of the conformers C_{fast}:C_{slow} and redox potential exists: the more reaction centers in the fast conformer, the more negative the redox

potential of Q_A. This model implies that the conformers have different redox potentials of Q_A and that reaction centers in the fast recombining state have a lower potential Q_A. It remains, however unclear what the actual redox potential of the single conformer is and how it contributes to the weighted average. A complex nonlinear behavior would not be surprising because the binding constants of the herbicides may differ in the two conformers and are certainly different when Q_A^- is present. Hence a mathematical description of a model would have to take at least eight reaction center states into account, fast and slow conformers, with and without inhibitor, and each state oxidized or reduced.

We undertook this study to obtain insights into herbicide functioning in PSII by studying plant herbicides in the better characterized reaction center of purple photosynthetic bacteria. The differential shifts of the redox potential of Q_A induced by the binding of bromoxynil or DCMU and the changes in the kinetics of the $P^{+\bullet}Q_A^{-\bullet}$ recombination that were found here in the bacterial reaction center are remarkably similar to those occurring in the PSII. In *Bl. viridis* we found that the main influence of the herbicides on the recombination kinetics is that they appeared to change the ratio of the phases of the biphasic $P^{+\bullet}Q_A^{-\bullet}$ decay kinetics rather than simply changing the rates of each phase. In bacterial reaction centers, this biphasicity has been linked to two different conformations that are in a slow equilibrium. The action of the herbicides can thus be seen as influencing the equilibrium constant for this conformation change. The question arises then whether herbicides could act in a similar way in PSII. The marked biphasic kinetics of charge recombination ($S_2Q_A^{-\bullet}$) could reflect a related conformational equilibrium in PSII. The existence of multiple conformers in PSII has also been suggested before (*54*, *55*). Our preliminary experiments investigating the $S_2Q_A^{-\bullet}$ recombination luminescence indicate that the herbicides do indeed alter the ratio of the biphasic kinetics (unpublished results).

The molecular origin of the fast and slow conformations has yet to be made clear. Even in the bacterial reaction center there is little to go on. However, it is possible that structural studies using methods such as X-ray crystallography, FTIR, or computational calculations done on reaction centers treated with these plant herbicides could help to understand the structural origin of the conformational states and how herbicides are able to influence their distribution.

ACKNOWLEDGMENT

We thank Drs. Pierre Sebban, Klaus Brettel, Winfried Leibl, Andreas Labahn, Eberhard Schlodder, and Pierre Sétif for stimulating discussions and Wolfgang Haehnel, Klaus Brettel, and Winfried Leibl for allowing us to do experiments on their equipment.

SUPPORTING INFORMATION AVAILABLE

One figure showing the fitting of the $P^{+\bullet}$ reduction with one, two, or three exponentials. This material is available free of charge via the Internet at http://pubs.acs.org.

REFERENCES

1. Hoff, A. J., and Deisenhofer, J. (1997) Photophysics of photosynthesis. Structure and spectroscopy of reaction centers of purple bacteria, *Phys. Rep. 287*, 1−247.
2. Okamura, M. Y., Paddock, M. L., Graige, M. S., and Feher, G. (2000) Proton and electron transfer in bacterial reaction centers. *Biochim. Biophys. Acta 1458*, 148−163.
3. Wraight, C. A. (2004) Proton and electron transfer in the acceptor quinone complex of photosynthetic reaction centers from *Rhodobacter sphaeroides*, *Front. Biosci. 9*, 309−337.
4. Lancaster, C. R., Bibikova, M. V., Sabatino, P., Oesterhelt, D., and Michel, H. (2000) Structural basis of the drastically increased initial electron transfer rate in the reaction center from a *Rhodopseudomonas viridis* mutant described at 2.00 Å resolution, *J. Biol. Chem. 275*, 39364−39368.
5. Fritzsch, G., Koepke, J., Diem, R., Kuglstatter, A., and Baciou, L. (2002) Charge separation induces conformational changes in the photosynthetic reaction centre of purple bacteria, *Acta Crystallogr., Sect. D: Biol. Crystallogr. 58*, 1660−1663.
6. Menin, L., Gaillard, J., Parot, P., Schoepp, B., Nitschke, W., and Vermeglio, A. (1998) Role of HiPIP as electron donor to the RC-bound cytochrome in photosynthetic purple bacteria, *Photosynth. Res. 55*, 343−348.
7. Shopes, R. J., and Wraight, C. A. (1985) The acceptor quinone complex of *Rhodopseudomonas viridis* reaction centers, *Biochim. Biophys. Acta 806*, 348−356.
8. Gopher, A., Blatt, Y., Schonfeld, M., Okamura, M. Y., Feher, G., and Montal, M. (1985) The effect of an applied electric field on the charge recombination kinetics in reaction centers reconstituted in planar lipid bilayers, *Biophys. J. 48*, 311−320.
9. Woodbury, N. W., Parson, W. W., Gunner, M. R., Prince, R. C., and Dutton, P. L. (1986) Radical-pair energetics and decay mechanisms in reaction centers containing anthraquinones, naphthoquinones or benzoquinones in place of ubiquinone, *Biochim. Biophys. Acta 851*, 6−22.
10. Dutton, P. L., Prince, R. C., and Tiede, D. M. (1978) The reaction center of photosynthetic bacteria, *Photochem. Photobiol. 28*, 939−949.
11. Rutherford, A. W. (1989) Photosystem II, the water-splitting enzyme, *Trends Biochem. Sci. 14*, 227−232.
12. Diner, B. A., and Babcock, G. T. (1996) Structure, dynamics, and energy conversion efficiency in photosystem II, in *Oxygenic Photosynthesis: The Light Reactions* (Ort, D. R., and Yocum, C. F., Eds.) pp 213−247, Kluwer, Dordrecht.
13. Velthuys, B. R. (1981) Electron-dependent competition between plastoquinone and inhibitors for binding to photosystem II, *FEBS Lett. 126*, 277−281.
14. Wraight, C. A. (1981) Oxidation-reduction physical chemistry of the acceptor quinone complex in bacterial photosynthetic reaction centers: Evidence for a new model of herbicide activity, *Isr. J. Chem. 21*, 348−354.
15. Krieger-Liszkay, A., and Rutherford, A. W. (1998) Influence of herbicide binding on the redox potential of the quinone acceptor in photosystem II: relevance to photodamage and phytotoxicity, *Biochemistry 37*, 17339−17344.
16. Rutherford, A. W., and Krieger-Liszkay, A. (2001) Herbicide-induced oxidative stress in photosystem II, *Trends Biochem. Sci. 26*, 648−653.
17. Johnson, G. N., Rutherford, A. W., and Krieger, A. (1995) A change in the midpotential of the quinon Q_A in the photosystem II associated with photoactivation of oxygen evolution, *Biochim. Biophys. Acta 1229*, 202−207.
18. Rappaport, F., Guergova-Kuras, M., Nixon, P. J., Diner, B. A., and Lavergne, J. (2002) Kinetics and pathways of charge recombination in photosystem II, *Biochemistry 41*, 8518−8527.
19. Rutherford, A. W., Paterson, D. R., and Mullet, J. E. (1981) A light-induced spin-polarized triplet detected by EPR in photosystem II reaction centers, *Biochim. Biophys. Acta 635*, 205−214.
20. Van Gorkom, H. J. (1985) Electron transfer in photosystem II, *Photosynth. Res. 6*, 97−112.
21. Durrant, J. R., Giorgi, L. B., Barber, J., Klug, D. R., and Porter, G. (1990) Characterisation of triplet states in isolated photosystem II reaction centres: Oxygen quenching as a mechanism for photodamage, *Biochim. Biophys. Acta 1017*, 167−175.
22. Macpherson, A. N., Telfer, A., Barber, J., and Truscott, T. G. (1993) Direct detection of singlet oxygen from isolated photosystem II reaction centres, *Biochim. Biophys. Acta 1143*, 301−309.
23. Hideg, É., Spetea, C., and Vass, I. (1994) Singlet oxygen production in thylakoid membranes during photoinhibition as detected by EPR spectroscopy, *Photosynth. Res. 39*, 191−199.
24. Keren, N., Berg, A., van Kan, P. J., Levanon, H., and Ohad, I. I. (1997) Mechanism of photosystem II photoinactivation and D1

protein degradation at low light: The role of back electron flow, *Proc. Natl. Acad. Sci. U.S.A. 94*, 1579−1584.
25. Telfer, A., Bishop, S. M., Phillips, D., and Barber, J. (1994) Isolated photosynthetic reaction center of photosystem II as a sensitizer for the formation of singlet oxygen. Detection and quantum yield determination using a chemical trapping technique, *J. Biol. Chem. 269*, 13244−13253.
26. Fufezan, C., Rutherford, A. W., and Krieger-Liszkay, A. (2002) Singlet oxygen production in herbicide-treated photosystem II, *FEBS Lett. 532*, 407−410.
27. Dutton, P. L., Leigh, J. S., and Wraight, C. A. (1973) Direct measurement of the midpoint potential of the primary electron acceptor in Rhodopseudomonas spheroides in situ and in the isolated state: some relationships with pH and o-phenanthroline, *FEBS Lett. 36*, 169−173.
28. Sinning, I., Michel, H., Mathis, P., and Rutherford, A. W. (1989) Characterization of four herbicide-resistant mutants of *Rhodopseudomonas viridis* by genetic analysis, electron paramagnetic resonance, and optical spectroscopy, *Biochemistry 28*, 5544−5553.
29. Spitz, J. A., Derrien, V., and Sebban, P. (2005) Specific triazine resistance in bacterial reaction centers induced by a single mutation in the Q_A protein pocket, *Biochemistry 44*, 1338−1343.
30. Baciou, L., and Sebban, P. (1995) Heterogeneity of the quinone electron-acceptor system in bacterial reaction centers, *Photochem. Photobiol. 62*, 271−278.
31. Rutherford, A. W. (1986) How close is the analogy between the reaction centre of photosystem II and that of purple bacteria?, *Biochem. Soc. Trans. 14*, 15−17.
32. Michel, H., and Deisenhofer, J. (1988) Relevance of the photosynthetic reaction center from purple bacteria to the structure of photosystem II, *Biochemistry 27*, 1−7.
33. Sinning, I., Michel, H., Mathis, P., and Rutherford, A. W. (1989) Terbutryn resistance in a purple bacterium can induce sensitivity toward the plant herbicide DCMU, *FEBS Lett. 256*, 192−194.
34. Sinning, I. (1992) Herbicide binding in the bacterial photosynthetic reaction center, *Trends Biochem. Sci. 17*, 150−154.
35. Lancaster, C. R., and Michel, H. (1999) Refined crystal structures of reaction centres from *Rhodopseudomonas viridis* in complexes with the herbicide atrazine and two chiral atrazine derivatives also lead to a new model of the bound carotenoid, *J. Mol. Biol. 286*, 883−898.
36. Drepper, F., Hippler, M., Nitschke, W., and Haehnel, W. (1996) Binding dynamics and electron transfer between plastocyanin and photosystem I, *Biochemistry 35*, 1282−1295.
37. Trosper, T. L., Benson, D. L., and Thornber, P. J. (1977) Isolation and spectral characteristics of the photochemical reaction center of *Rhodopseudomonas viridis*, *Biochim. Biophys. Acta 460*, 318−330.
38. Gibasiewicz, W., Brettel, K., Dobek, A., and Leibl, W. (1999) Reexamination of primary radical pair recombination in *Rps. viridis* with Q_A reduced, *Chem. Phys. Lett. 315*, 95−102.
39. Stein, R. R., Castellvi, A. L., Bogacz, J. P., and Wraight, C. A. (1984) Herbicide-quinone competition in the acceptor complex of photosynthetic reaction centers from *Rhodopseudomonas sphaeroides*: a bacterial model for PS-II-herbicide activity in plants, *J. Cell. Biochem. 24*, 243−259.
40. Kleinfeld, D., Okamura, M. Y., and Feher, G. (1984) Electron-transfer kinetics in photosynthetic reaction centers cooled to cryogenic temperatures in the charge-separated state: evidence for light-induced structural changes, *Biochemistry 23*, 5780−5786.
41. Shuvalov, V. A., and Parson, W. W. (1981) Triplet states of monomeric bacteriochlorophyll in vitro and of bacteriochlorophyll dimers in antenna and reaction center complexes, *Biochim. Biophys. Acta 638*, 50−59.
42. Shopes, R. J., and Wraight, C. A. (1987) Charge recombination from the $P^+Q_A^-$ state in reaction centers from *Rhodopseudomonas viridis*, *Biochim. Biophys. Acta 893*, 409−425.
43. Parot, P., Thiery, J., and Verméglio, A. (1987) Charge recombination at low temperature in photosynthetic bacteria reaction centers: Evidence for two conformation states, *Biochim. Biophys. Acta 893*, 534−543.
44. Sebban, P. (1988) pH effect on the biphasicity of the $P^+Q_A^-$ charge recombination kinetics in the reaction centers from *Rhodobacter sphaeroides*, reconstituted with anthraquinones, *Biochim. Biophys. Acta 936*, 128−132.
45. Sebban, P., and Wraight, C. A. (1989) Heterogeneity of the $P^+Q_A^-$ recombination kinetics in reaction centers from *Rhodopseudomonas viridis*: the effects of pH and temperature, *Biochim. Biophys. Acta 974*, 54−65.
46. Sebban, P., Parot, P., Baciou, L., Mathis, P., and Verméglio, A. (1991) Effects of low temperature and lipid rigidity on the charge recombination process in *Rps. viridis* and *Rb. sphaeroides* reaction centers, *Biochim. Biophys. Acta 1057*, 109−114.
47. Schoepp, B., Parot, P., Lavorel, J., and Verméglio, A. (1992) Charge recombination kinetics in bacterialphotosynthetic reaction centers: conformational states in equilibrium pre-exist in the dark, in *The Photosynthetic Bacterial Reaction Center: Structure, Spectroscopy, and Dynamics* (Breton, J., and Verméglio, A., Eds.) pp 331−339, Plenum Press, London.
48. Baciou, L., Rivas, E., and Sebban, P. (1990) $P^+Q_A^-$ and $P^+Q_B^-$ charge recombinations in *Rhodopseudomonas viridis* chromatophores and in reaction centers reconstituted in phosphatidylcholine liposomes. Existence of two conformational states of the reaction centers and effects of pH and o-phenanthroline, *Biochemistry 29*, 2966−2976.
49. Gao, J.-L., Shopes, R. J., and Wraight, C. (1991) Heterogeneity of kinetics and electron transfer equilibria in the bacteriopheophytin and quinone electron acceptors of reaction centers from *Rhodopseudomonas viridis*, *Biochim. Biophys. Acta 1056*, 259−272.
50. Marcus, R. A., and Sutin, N. (1985) Electron transfers in chemistry and biology, *Biochim. Biophys. Acta 811*, 265−322.
51. Holten, D., Windsor, M. W., Parson, W. W., and Thornber, J. P. (1978) Primary photochemical processes in isolated reaction centers of *Rhodopseudomonas viridis*, *Biochim. Biophys. Acta 501*, 112−126.
52. Prince, R. C., Leigh, J. S., Jr., and Dutton, P. L. (1976) Thermodynamic properties of the reaction center of *Rhodopseudomonas viridis*, *Biochim. Biophys. Acta 440*, 622−636.
53. Cogdell, R. J., and Crofts, A. R. (1972) Some observations on the primary acceptor of *Rhodopseudomonas viridis*, *FEBS Lett. 27*, 176−178.
54. Trebst, A., Depka, B., Kraft, B., and Johanningmeier, U. (1988) The Q_B site modulates the conformation of the photosystem II reaction center polypeptides, *Photosynth. Res. 18*, 163−177.
55. Rappaport, F., Cuni, A., Xiong, L., Sayre, R. T., and Lavergne, J. (2005) Charge recombination and thermoluminescence in photosystem II, *Biophys. J. 88*, 1948−1958.

BI050055J